

pubs.acs.org/JPCA Article

# Comparison of Variational and Perturbative Spin—Orbit Coupling within Two-Component CASSCF

Published as part of The Journal of Physical Chemistry A virtual special issue "Roland Lindh Festschrift".

Can Liao, Chad E. Hoyer, Rahoul Banerjee Ghosh, Andrew J. Jenkins, Stefan Knecht, Michael J. Frisch, and Xiaosong Li\*



Cite This: J. Phys. Chem. A 2024, 128, 2498-2506



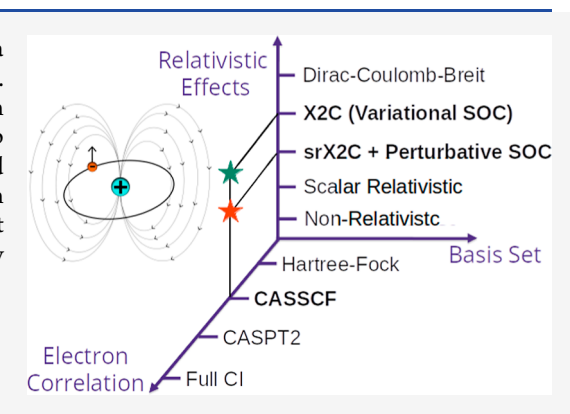
**ACCESS** 

Metrics & More

Article Recommendations

s Supporting Information

**ABSTRACT:** The modeling of spin—orbit coupling (SOC) remains a challenge in computational chemistry due to the high computational cost. With the rising popularity of spin-driven processes and f-block metals in chemistry and materials science, it is incumbent on the community to develop accurate multiconfigurational SOC methods that scale to large systems and understand the limits of different treatments of SOC. Herein, we introduce an implementation of perturbative SOC in scalar-relativistic two-component CASSCF (srX2C-CASSCF-SO). Perspectives on the limitations and accuracy of srX2C-CASSCF-SO are presented via benchmark calculations.



#### 1. INTRODUCTION

Some of the biggest challenges in modeling the spectroscopy of late transition and f-block metals are their multireference nature and the presence of spin—orbit coupling (SOC). These same challenges also make them viable candidates to fill many roles in chemistry and materials science such as catalysis, <sup>1–5</sup> quantum information technology, <sup>6</sup> and solar cell technology. <sup>7–9</sup> The complete active space self-consistent field (CASSCF) method is usually the computational framework for treating multireference effects. <sup>10</sup> For capturing SOC, two approaches are available: perturbative or variational.

Perturbation theory is the most popular approach to address SOC.  $^{11-30}$  This method starts by variationally obtaining a set of zeroth-order states in the absence of SOC and subsequently introducing SOC via first-order perturbation theory. This is also known as a state interaction. First-order perturbation theory is valid for small perturbations, but it is unclear at what point does SOC become too large and variational methods become necessary, for example, see the open question of the chemical bonding in the early actinide dimer  $\rm U_2$ .  $^{31-33}$ 

Variational methods provide the most complete description of SOC. These methods employ the Dirac Hamiltonian and self-consistently optimize orbitals with SOC in consideration. The full Dirac Hamiltonian requires computationally expensive complex-valued four-component non-collinear spinor wave function. Approximations to the Dirac Hamiltonian such as the exact two-component (X2C) Hamiltonian have shown success in capturing scalar relativity and

SOC. <sup>51–53,56–59,61–77</sup> To capture SOC variationally, the X2C method still requires orbitals to be described by expensive complex-valued four-component non-collinear spinor wave functions. It should also be noted that an approximate variational SOC method was developed by Neese and Ganyushin. <sup>78</sup> In this method, one-component spin-aligned orbitals are optimized in the presence of SOC during MCSCF. CI coefficients are allowed to be complex; however, orbital coefficients are strictly real-valued.

The perturbative SOC approach has been developed within the one-component spin-aligned state-averaged CASSCF formalism.  $^{15,79,80}$  This is widely referred to as CASSCF-SO. Building a suitable SOC Hamiltonian requires coupling between different spin eigenstates (e.g., S=0, 1) and their microstates (e.g.,  $M_S=-1$ , 0, and 1 in S=1). Obtaining a full set of spin microstates requires including spin-flipped configurations in the CASSCF calculation. Typically, one-component spin-aligned CASSCF does not include spin-flipped configurations and consequently does not organically yield the complete set of spin microstates needed to fully form the SOC Hamiltonian. To obtain the missing microstate

Received: December 7, 2023 Revised: February 21, 2024 Accepted: February 28, 2024 Published: March 15, 2024





information, one must invoke the Wigner–Eckart theorem. Furthermore, the Wigner–Eckart theorem requires spin eigenstates, which can be obtained using a configuration state function (CSF) basis. <sup>15,29,81</sup> In a CSF basis, different spin eigenstates are obtained through independent CASSCF calculations, making the workflow of the calculation unwieldy, especially if a large number of spin manifolds are required to accurately span the SOC Hamiltonian. Additionally, independent CASSCF calculations cause the orbitals between different spin states to be nonorthogonal. Before constructing the SOC Hamiltonian, the nonorthogonality must be reconciled through a biorthogonalization procedure. <sup>15,82</sup>

In this work, we introduce an implementation of perturbative SOC and move toward determining its limits. The zeroth-order states in this implementation arise from onecomponent scalar relativistic spin-aligned CASSCF. Relativistic effects are included using the exact two-component (X2C) Hamiltonian, which leads us to refer to this implementation as srX2C-CASSCF-SO. This implementation offers the advantage of forgoing the need for CSFs, the Wigner-Eckart theorem, and biorthogonalization by including spin-flipped configurations in a streamlined manner. The need for multiple independent CASSCF calculations is reduced to one CASSCF calculation with a subsequent real-valued two-component CASCI calculation to generate the interaction space. This implementation is benchmarked against the widely used CSFbased implementation of CASSCF-SO available in the quantum chemistry software package OpenMolCAS, 15,83,84 a variational SOC method, 52,77 and experimental results for various atoms along with a diatomic test case.

## 2. METHODS

**2.1. Variational Spin–Orbit Coupling in CASSCF.** We approach variational SOC through the exact two-component  $(X2C)^{51,53,56,58,59,61-76}$  transformation of the Dirac equation. We refer readers to ref 77 for detailed implementation of X2C-CASSCF. In this section, we only present a brief theory background to lay the foundation for the perturbative treatment of SOC in the two-component framework. The matrix representation of the modified one-electron Dirac equation under restricted kinetic balance is shown in eq 1

$$\begin{pmatrix}
\mathbf{V} & \mathbf{T} \\
\mathbf{T} & \frac{1}{4c^2}\mathbf{W} - \mathbf{T}
\end{pmatrix}
\begin{pmatrix}
\mathbf{C}_{L}^{+} & \mathbf{C}_{L}^{-} \\
\mathbf{C}_{S}^{+} & \mathbf{C}_{S}^{-}
\end{pmatrix}$$

$$= \begin{pmatrix}
\mathbf{S} & \mathbf{0}_{2} \\
\mathbf{0}_{2} & \frac{1}{2c^2}\mathbf{T}
\end{pmatrix}
\begin{pmatrix}
\mathbf{C}_{L}^{+} & \mathbf{C}_{L}^{-} \\
\mathbf{C}_{S}^{+} & \mathbf{C}_{S}^{-}
\end{pmatrix}
\begin{pmatrix}
\epsilon^{+} & \mathbf{0}_{2} \\
\mathbf{0}_{2} & \epsilon^{-}
\end{pmatrix}$$
(1)

where c is the speed of light and V, T, and S are the two-component nonrelativistic potential energy, kinetic energy, and overlap matrices, respectively.  $\epsilon^{\pm}$  are the positive/negative eigenvalues corresponding to molecular orbitals represented by the coefficients  $C_L^{\pm}$  and  $C_S^{\pm}$ .

The relativistic potential matrix W is

$$\mathbf{W} = (\boldsymbol{\sigma} \cdot \mathbf{p}) \mathbf{V} (\boldsymbol{\sigma} \cdot \mathbf{p})$$

$$= \mathbf{p} \mathbf{V} \cdot \mathbf{p} + i \boldsymbol{\sigma} \cdot \mathbf{p} \mathbf{V} \times \mathbf{p}$$

$$= \mathbf{W}_{sr} + \mathbf{W}_{sd}$$
(2)

where  $\sigma$  is the vector of Pauli spin matrices and  $\mathbf{p}$  is the linear momentum operator. This relativistic potential term can be

spin-separated using the Dirac identity into a scalar relativistic term (sr) and spin-dependent (sd) term.<sup>85,86</sup>

The X2C technique allows us to reduce the dimension of the problem by block-diagonalizing the Hamiltonian via a unitary transformation that "folds" the small-component wave function into a pseudo-large component so that the four-component Dirac equation becomes an effective two-component eigenvalue problem.

$$\begin{pmatrix} \mathbf{U}^{LL,\dagger} & \mathbf{U}^{SL,\dagger} \\ \mathbf{U}^{LS,\dagger} & \mathbf{U}^{SS,\dagger} \end{pmatrix} \begin{pmatrix} \mathbf{V} & \mathbf{T} \\ \mathbf{T} & \frac{1}{4c^2} \mathbf{W} - \mathbf{T} \end{pmatrix} \begin{pmatrix} \mathbf{U}^{LL} & \mathbf{U}^{LS} \\ \mathbf{U}^{SL} & \mathbf{U}^{SS} \end{pmatrix}$$
$$= \begin{pmatrix} \mathbf{H}^{+}_{X2C} & 0 \\ 0 & \mathbf{H}^{-}_{X2C} \end{pmatrix}$$
(3)

For most chemical systems, formulating the electronic structure theory using the Hamiltonian  $\mathbf{H}_{X2C}^+$  that corresponds to the positive energy solutions is sufficient. For the sake of brevity, we refer to  $\mathbf{H}_{X2C}^+$  as  $\mathbf{H}$ . In this implementation, only one-electron operators are included in the X2C transformation. The two-electron Coulomb operator is included without picture change after the transformation.

The two-electron spin—orbit operator is approximated using the row-dependent Dirac-Coulomb-Breit-parametrized screened-nuclear spin-orbit (SNSO) factor. 87,88 Compared to the original SNSO approximation, which is based on an empirical observation,<sup>87</sup> the row-dependent Dirac-Coulomb-Breit-parametrized SNSO has been extensively evaluated and demonstrates a remarkably low average error of only 0.4% in orbital splittings across the entire periodic table.<sup>88</sup> This is in contrast to the atomic-mean-field method, 11,15,89 which, although it employs the exact atomic two-electron spin-orbit interaction, sacrifices the variational optimization of the full atomic density. In the Dirac-Coulomb-Breit-parametrized SNSO, one-electron spin-orbit interaction is designed to support variational calculations within the X2C relativistic framework. For the purpose of making a clear and consistent comparison with the variational X2C relativistic method, we chose to adopt the same spin-orbit coupling approximation.

**2.2. CASSCF State Interaction with Perturbative SOC.** Based on the spin-separation scheme in eq 2, the X2C Hamiltonian can be written as

$$\mathbf{H} = \mathbf{H}_{sr} + \mathbf{H}_{sd}$$

$$\mathbf{H}_{sr} = (\mathbf{U}^{LL,\dagger} \mathbf{U}^{SL,\dagger}) \begin{pmatrix} \mathbf{V} & \mathbf{T} \\ \mathbf{T} & \frac{1}{4\epsilon^2} \mathbf{p} \mathbf{V} \cdot \mathbf{p} - \mathbf{T} \end{pmatrix} (\mathbf{U}^{LL} \mathbf{U}^{SL})$$

$$\mathbf{H}_{sd} = (\mathbf{U}^{LL,\dagger} \mathbf{U}^{SL,\dagger}) \begin{pmatrix} 0 & 0 \\ 0 & \frac{1}{4\epsilon^2} i\boldsymbol{\sigma} \cdot \mathbf{p} \mathbf{V} \times \mathbf{p} \end{pmatrix} (\mathbf{U}^{LL} \mathbf{U}^{SL})$$

The first term is a product of spatial operators, which carries the symmetry of a rank 0 tensor, contracted with scalar densities. As a result, the first term can be effectively formulated in a real-value spin-aligned one-component approach. The second term couples the spin and spatial operators, giving rise to the spin- and orbit-dependent interactions, including the spin—orbit term. However, the spin-dependent term requires a computational framework in complex-valued non-collinear two- or four-component basis.

When spin-orbit coupling is relatively weak compared to the orbital energy gap, it can be effectively treated with a

Table 1. Mean and Maximum Absolute Error of Atomic Excitation Energies (in eV) for CASSCF-SO, srX2C-CASSCF-SO, and X2C-CASSCF<sup>a</sup>

	mean AE	max AE	average exp splitting
4d (Y, Zr, Nb, Ru, Rh)			0.083
CASSCF-SO <sup>b</sup>	0.008	0.034	
srX2C-CASSCF-SO <sup>c</sup>	0.012	0.041	
X2C-CASSCF <sup>c</sup>	0.011	0.030	
5d (Hf, Ta, W, Os, Ir)			0.223
CASSCF-SO	0.144 (0.042)	0.778 (0.114)	
srX2C-CASSCF-SO	0.149 (0.053)	0.790 (0.095)	
X2C-CASSCF	0.141 (0.066)	0.711 (0.094)	
<b>5p</b> (In, Sn, Te, I)			0.372
CASSCF-SO	0.047	0.080	
srX2C-CASSCF-SO	0.048	0.083	
X2C-CASSCF	0.034	0.053	
<b>6p</b> (Tl, Pb, Po)			0.875
CASSCF-SO	0.195	0.309	
srX2C-CASSCF-SO	0.212	0.346	
X2C-CASSCF	0.187	0.340	
4f (Pr, Nd, Pm, Sm, Dy, Ho, Tm)			0.233
CASSCF-SO	0.034	0.110	
srX2C-CASSCF-SO	0.043	0.126	
X2C-CASSCF	0.014	0.076	
<b>5f</b> (U <sup>3+</sup> , Np <sup>3+</sup> , Pu <sup>3+</sup> )			0.215
CASSCF-SO	0.219	0.666	
srX2C-CASSCF-SO	0.246	0.644	
X2C-CASSCF <sup>d</sup>	0.208	0.614	

"The table is divided into blocks of the periodic table (4d, 5d, 5p, etc.). Errors for the 5d block with Os and Ir omitted are placed in parentheses. The average experimental splitting is defined as the average energy difference between adjacent *J*-states. All calculations were performed using the ANO-RCC basis set. 33,94 Absolute error (AE) is defined as the unsigned difference between the computed value and the experimental value. Excitation energies for individual atoms are recorded in the Supporting Information. Atomic-mean-field two-electron integrals are used. Dirac—Coulomb—Breit-parametrized row-dependent screened-nuclear spin—orbit scaling is used. State-averaged over the first *J*-manifold.

perturbative approach by way of first-order perturbation theory, also known as state interaction.  $^{15,83}$  In this approach, the scalar-relativistic Hamiltonian  $\mathbf{H}_{\rm sr}$  can be used as the zeroth-order Hamiltonian. The spin-dependent Hamiltonian  $\mathbf{H}_{\rm sd}$  is introduced as a perturbation expanded in the basis of zeroth-order wave functions, called the interaction space, resulting in SOC-perturbed Hamiltonian  $\mathbf{H}'$ . The eigenvalues of  $\mathbf{H}'$  are the SOC-perturbed state energies, and the resulting eigenstates are spin—orbit adiabatic states expressed as a linear combination of the zeroth-order states.

The spin—orbit matrix elements between zeroth-order states  $|I\rangle$  and  $|I\rangle$  are

$$[\mathbf{H}_{so}]_{IJ} = \sum_{pq} \gamma_{pq}^{IJ} [\mathbf{H}_{sd}]_{pq}$$
(5)

where  $\gamma_{pq}^{IJ}$  is the one-particle scalar transition density matrix between states  $|I\rangle$  and  $|J\rangle$  or one-particle reduced density matrix for  $|I\rangle = |J\rangle$ . p and q are spatial orbital indices.

In this work, we seek to obtain all spin states and their microstates in a fully orthogonal space to aid in the automatic construction of the state interaction Hamiltonian  $\mathbf{H}_{so}$ . This is done through constructing a two-component spin-aligned spinor basis from scalar-relativistic one-component CASSCF orbitals, followed by a scalar-relativistic X2C-CASCI (srX2C-CASCI) calculation to yield a full set of spin eigenstates and spin microstates used to construct  $\mathbf{H}_{so}$ . The construction of the two-component spin-aligned spinor basis is shown in eq 6. For every one-component spin-aligned spatial orbital, a Kramers

pair of two-component spin-aligned spinors was constructed by using the spatial orbital.

$$\{\phi_i\} \to \left\{ \begin{pmatrix} \phi_i \\ 0 \end{pmatrix}, \begin{pmatrix} 0 \\ \phi_i \end{pmatrix} \right\}$$
 (6)

In the absence of an external magnetic field that can split spin microstates, the state interaction Hamiltonian obtained from CASSCF-SO using biorthogonal CSF and Wigner—Eckart theory is identical to those from the srX2C-CASSCF-SO. The advantage of using a one-component to two-component construction is to automate the CASSCF-SO procedure and to allow for scenarios where Kramers' symmetry is broken, e.g., in an external magnetic field.

## 3. RESULTS AND DISCUSSION

Both variational X2C-CASSCF and perturbative srX2C-CASSCF-SO methods are implemented in a development version of the Gaussian quantum chemistry software package. The workflow of the perturbative srX2C-CASSCF-SO calculation is as follows:

- 1. Perform Hartree-Fock calculation.
- 2. Perform scalar-relativistic one-component CASSCF using Hartree—Fock canonical orbitals as a reference.
- 3. Construct two-component spin-aligned spinor basis from one-component spin-aligned CASSCF orbitals and perform an srX2C-CASCI.

4. Form  $\mathbf{H}_{so}$  and the SOC-perturbed  $\mathbf{H}'$  within the interaction space and diagonalize  $\mathbf{H}'$  to obtain spinorbit adiabatic states.

CSF-based CASSCF-SO calculations were also carried out using OpenMolCAS $^{84}$  to assess the accuracy of different perturbative SOC implementations.

In the variational X2C-CASSCF and perturbative srX2C-CASSCF-SO methods, the two-electron spin—orbit effect is approximated using the row-dependent Dirac—Coulomb—Breit-parametrized screened-nuclear spin—orbit factor. <sup>87,88</sup> In the CSF-based CASSCF-SO calculations, the second-order Douglas—Kroll—Hess (DKH) Hamiltonian was used to describe scalar relativistic effects while one-electron spin—orbit effects were included perturbatively via the DKH Hamiltonian spin—orbit operator. <sup>15,91</sup> Additionally, the two-electron spin—orbit effect is approximated via the atomic-mean-field (AMFI) approach with the Dirac—Coulomb operator. <sup>11,15,89</sup>

3.1. Atomic Fine-Structure Splitting. In this section, the accuracy of CASSCF-SO, srX2C-CASSCF-SO, and X2C-CASSCF was compared for atomic cases. We compared the excitation energies of all J-manifolds arising from the lowest term due to fine-structure splitting. All systems used in the benchmark had a partially filled valence subshell configuration. For each atom, the active space comprised all valence orbitals. For example, Pr is in the 4f-block and has a partially filled valence subshell configuration of 4f3. The active space for Pr comprises 14 orbitals (7 alpha and 7 beta orbitals for spinaligned calculations) and 3 electrons, where all 14 orbitals were 4f orbitals. All CASSCF states arising from the active space were included in the interaction space. The details of individual calculations are found in the Supporting Information. Experimental results were obtained from the NIST Atomic Spectra Database and other work found in the literature.

Table 1 shows the mean and maximum absolute errors of each method with respect to blocks of the periodic table. The error for each method increases as atomic number increases. In these benchmark calculations, the difference in accuracy between the two perturbative methods, CASSCF-SO and srX2C-CASSCF-SO, is small, in the range of 1–27 meV, with CASSCF-SO being the more accurate approach. Calculations without the consideration of two-electron spin—orbit coupling show that the difference is mainly due to the different two-electron spin—orbit approximations employed. For atomic fine-structure splitting, it appears that the atomic-mean-field approach is slightly more accurate than the screened-nuclear spin—orbit approximation. These results are listed in the Supporting Information.

Although X2C-CASSCF outperformed the perturbative methods in mean absolute error in all blocks except for the 4d-block, the errors between X2C-CASSCF and srX2C-CASSCF-SO only differing on the order of 1–38 meV. Errors are significantly higher for the 5d, 6p, and 5f-blocks. These errors have been previously observed in both perturbative and variational methods and can be improved with more dynamic correlation. Omitting the highly correlated cases in the 5d block (Os and Ir) significantly reduced the mean and max absolute errors which suggests that highly correlated methods are required for atoms with Z > 75.

Figure 1 shows the mean absolute error of srX2C-CASSCF-SO and X2C-CASSCF ground state fine-structure splitting,

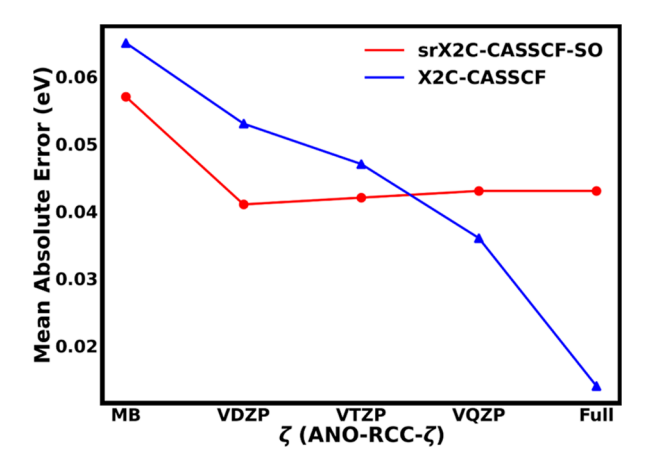


**Figure 1.** Mean absolute error (eV) of the ground-state fine-structure splitting for the 4f-block using srX2C-CASSCF-SO and X2C-CASSCF was plotted as a function of basis set  $\zeta$ .

approaching the basis set limit for the 4f-block. Basis set convergence behavior has been studied in previous work for perturbative spin—orbit coupling<sup>95</sup> but has not been compared to variational spin-orbit approaches. Improvement was seen in both srX2C-CASSCF-SO and X2C-CASSCF when the basis was improved from the minimal basis (MB) to double-\(\zeta\) (VDZP). Improving the basis had a negligible effect past VDZP on srX2C-CASSCF-SO, whereas X2C-CASSCF showed systematic improvement. In the variational approach, the spin-orbit operator is applied at the SCF level and is represented on the entire orbital basis. In the perturbative approach, the spin-orbit operator is represented in the interaction space, which is limited by the active space. The initial improvement seen in both approaches was due to the improved description of the 4f orbitals. However, increasing the basis set size past VDZP does not significantly improve the description of the 4f orbitals. Because the perturbative spinorbit operator is represented within the active space of only 4f orbitals, without improvement of the 4f orbitals, increasing the basis size minimally affected perturbative results. On the other hand, variational results continued to improve since the variational spin-orbit operator is not restricted by the active space. Further investigation into the behavior of perturbative and variational SOC methods with respect to active space is needed to thoroughly understand the basis set convergence behavior.

**3.2. Dependence of Fine-Structure Splitting of NdO**<sup>+</sup> **on Interaction Space.** At the full CI limit, when the interaction space encompasses all zeroth-order states, the perturbative and variational results should be identical. Within the CASSCF level of theory, the best representation of the spin—orbit Hamiltonian for a given active space is constructed from an interaction space that encompasses all zeroth-order CASSCF states. The results of the atomic benchmark were somewhat misleading in the sense that we only show the ideal cases where we can afford to utilize the maximum interaction space. In this section, we explore the behavior of perturbative SOC as a function of interaction space.

At the CASSCF level of theory, low-lying excited states of NdO<sup>+</sup> exist in a dense manifold of 52 states. A spin-free treatment of these states yield a set of multiplets spanning  $\sim 0.17$  eV. With SOC in consideration, these multiplets split into degenerate Kramers pairs spanning  $\sim 1.00$  eV. The bond length of NdO<sup>+</sup> was set to 1.742 Å, which was optimized at the

Table 2. Excitation Energies (in eV) for Low-Lying Excited States of NdO<sup>+</sup> for Various Interaction Spaces of Size N<sup>a</sup>

$J_{\mathrm{a}}$	Ω	srX2C-CASSCF-SO				X2C-CASSCF	Exp		
		N = 22	N = 36	N = 52	N = 68	N = 86	N = 364		
4.5	4.5	0.000	0.000	0.000	0.000	0.000	0.000	0.000	0.000
4.5	3.5	0.174	0.144	0.118	0.161	0.115	0.115	0.115	0.159
4.5	2.5	0.281	0.219	0.156	0.199	0.152	0.151	0.151	0.191
4.5	1.5	0.368	0.243	0.159	0.201	0.154	0.154	0.154	0.201
4.5	0.5	0.453	0.341	0.161	0.203	0.156	0.156	0.155	0.213
5.5	5.5	0.530	0.367	0.224	0.250	0.252	0.252	0.251	0.228
5.5	4.5	0.608	0.378	0.322	0.365	0.348	0.349	0.348	0.366
5.5	3.5	0.690	0.517	0.359	0.401	0.385	0.385	0.384	0.401
5.5	2.5	0.701	0.563	0.373	0.416	0.399	0.400	0.399	
5.5	1.5	0.749	0.596	0.376	0.419	0.402	0.403	0.403	
5.5	0.5	0.793	0.609	0.377	0.419	0.403	0.403	0.403	
mean AE	0.235	0.110	0.016	0.025	0.000	0.000			
max AE	0.390	0.206	0.027	0.048	0.001	0.001			

<sup>&</sup>lt;sup>a</sup>Absolute error (AE) in this table is defined as the unsigned difference between the perturbative srX2C-CASSCF-SO result and X2C-CASSCF. The ground state error was omitted from the mean AE.

CASSCF level of theory in a previous work.<sup>96</sup> The active space was chosen to be 3 electrons and 14 spin orbitals for srX2C-CASSCF-SO and X2C-CASSCF. Orbitals with majority 4f character were chosen to be in the active space. Calculations were state averaged over the lowest 52 states, which were all included in the interaction space. The ANO-RCC-VQZP basis set <sup>93,94</sup> was used in these calculations.

Table 2 shows excitation energies for low-lying states of NdO+ calculated using srX2C-CASSCF-SO and X2C-CASSCF as well as their experimental excitation energies. State notations were adapted from ref 96, where  $J_{\rm a}$  designate the total electronic angular momentum of the atomic ion and  $\Omega$  labels the unsigned projection of  $J_{\rm a}$  on the internuclear axis. We define the absolute error (AE) to be the unsigned difference between the srX2C-CASSCF-SO and X2C-CASSCF results for each computed state. Mean and maximum AEs are also recorded in Table 2. The lowest few experimentally observed states were included as a reference. Results with interaction spaces of sizes 86 < N < 364 are recorded in the Supporting Information.

We begin with the minimum interaction space required to recover the first two  $J_a$  manifolds, N=22. We increase then the interaction space by adding states in energetic order. The maximum interaction space size is N=364 states. Recovering excitation energies that rival the accuracy of X2C-CASSCF, the interaction space must encompass at least the lowest 86 spin-free states. In cases in which we are interested in a large number of states with strong spin—orbit coupling, such as simulating X-ray absorption spectra, it may be more convenient and cost-effective to use variational methods.

In Table 2, only interaction spaces that preserved the Kramers degeneracy of the  $(J_a, \Omega)$  manifolds were shown. Table 3 shows perturbative SOC energies resulting from inadequate interaction spaces. Interaction spaces where degenerate manifolds are partially included yield solutions with nonphysical degeneracy breaking.

The low-lying  $J_a$  manifolds of NdO<sup>+</sup> are  $J_a = 4.5$ , 5.5, 6.5, and 7.5, where each  $J_a$  manifold has 10, 12, 14, and 16 microstates, respectively. An interaction space of N = 34 omits two states from the  $J_a = 6.5$  manifold as well as two states from an 8-fold spin-free degeneracy. This caused degeneracy breaking between Kramers pairs in the  $J_a = 4.5$  manifold on the order

Table 3. Excitation Energies (in eV) for Low-Lying Excited States of NdO<sup>+</sup> for Various Inadequate Interaction Spaces That Lead to Unphysical Degeneracy Breaking<sup>a</sup>

			_	
$J_{\rm a}$	Ω	N = 24	N = 34	N = 51
4.5	4.5	0.000	0.000	0.000
		0.000	0.000	0.000
4.5	3.5	0.179	0.141	0.118
		0.179	0.141	0.119
4.5	2.5	0.291	0.214	0.156
		0.291	0.224	0.156
4.5	1.5	0.382	0.224	0.159
		0.382	0.307	0.160
4.5	0.5	0.470	0.326	0.161
		0.470	0.326	0.196
5.5	5.5	0.559	0.346	0.224
		0.561	0.346	0.224
5.5	4.5	0.564	0.361	0.322
		0.567	0.364	0.322
5.5	3.5	0.654	0.475	0.359
		0.654	0.475	0.363
5.5	2.5	0.740	0.531	0.373
		0.740	0.559	0.373
5.5	1.5	0.762	0.559	0.376
		0.762	0.568	0.376
5.5	0.5	0.804	0.568	0.377
		0.804	0.633	0.475

<sup>&</sup>lt;sup>a</sup>Kramers pairs with degeneracy breaking greater than 1 meV are in bold.

of 10 meV. Kramers degeneracy breaking was observed on the order of 1 meV in the  $J_a=6.5$  manifold when an interaction space of N=24, which includes only two states from the  $J_a=6.5$  manifold without the partial inclusion of spin-free degeneracies. Kramers degeneracy breaking was not observed for the N=22 interaction space, where no states were excluded from  $J_a$  manifolds, and two states were excluded from an 8-fold spin-free degeneracy. Furthermore, excluding a single complement to a Kramers pair also yields degeneracy breaking up to 98 meV, as demonstrated by interaction space N=51.

Our analysis shows that an appropriate interaction space is imperative for sound results. Not only does an incomplete interaction space yield erroneous energies, but it can also misrepresent the physics of the systems. One must be cautious when employing perturbative SOC and ensure that the interaction space has reached convergence, or at the very least, cover the symmetry of the system.

## 4. CONCLUSIONS

In this work, a perturbative SOC method was developed within the scalar-relativistic exact two-component CASSCF (srX2C-CASSCF-SO) framework via first-order perturbation theory. In the srX2C-CASSCF-SO implementation, one-component spinaligned scalar-relativistic CASSCF orbitals were used to construct a two-component spin-aligned spinor basis. This spinor basis was used in a srX2C-CASCI calculation to yield a full set of spin eigenstates and spin microstates to construct the spin—orbit Hamiltonian.

In our atomic benchmarks, the perturbative srX2C-CASSCF-SO methods were also compared to those of X2C-CASSCF, a variational SOC method. X2C-CASSCF outperformed or at the very least matched the performance of the perturbative methods. The difference in variational and perturbative SOC results only differed in the range of 1–27 meV. The difference in the perturbative results was mainly due to the differences in the treatment of two-electron spin—orbit coupling.

Preliminary results on the difference in the basis set convergence behavior between srX2C-CASSCF-SO and X2C-CASSCF were presented. The increase in basis size systematically improved X2C-CASSCF results, while srX2C-CASSCF-SO results remain largely unaffected past double- $\zeta$  quality. This study explores the behavior of the fine-structure splitting of low-lying excited states only for atomic lanthanide cases. More work is needed to draw definitive conclusions on the basis set convergence behavior of perturbative and variational methods.

Using the computed results for low-lying states of  $NdO^+$ , we have shown that the interaction space limit can be reached using a subspace of the maximum interaction space. When choosing a truncated interaction space, one must include enough states while preserving the symmetries of the system to recover degeneracies.

The aim of this research is to develop a scalable multireference method capable of accurately reproducing and predicting spectral properties in systems with significant spin—orbit coupling (SOC). We also aim to shed light on the limitations associated with variational and perturbative treatments of SOC. Our approach, termed srX2C-CASSCF-SO, utilizes a two-component spinor framework, which is automated to eliminate the necessity for configuration state functions (CSFs), the Wigner–Eckart theorem, and biorthogonalization procedures through a streamlined inclusion of spin-flipped configurations. Furthermore, the method can be readily extended to account for additional couplings introduced by the Breit operator, thereby including vector forms of spin–spin and orbit–orbit interactions.

In contrast to the CSF-based CASSCF-SO method, which requires *N* distinct CASSCF calculations for *N* spin states in the interaction space, followed by a biorthogonalization process, our proposed method involves only a single one-component CASSCF calculation and a real-valued two-component CASCI to construct the interaction space. Furthermore, the srX2C-CASSCF-SO approach is entirely formulated on real-valued arithmetic, resulting in a 6-fold

reduction in the computational cost for the CI segment compared to the complex-valued variational X2C-CASSCF method.

## ASSOCIATED CONTENT

#### Supporting Information

The Supporting Information is available free of charge at https://pubs.acs.org/doi/10.1021/acs.jpca.3c08031.

Supporting Information includes definitions of active space, state-average schemes, computed atomic excitation energies with and without two-electron spin—orbit coupling, and NdO<sup>+</sup> excitation energies (PDF)

## AUTHOR INFORMATION

## **Corresponding Author**

Xiaosong Li — Department of Chemistry, University of Washington, Seattle, Washington 98195, United States; orcid.org/0000-0001-7341-6240; Email: xsli@uw.edu

#### **Authors**

Can Liao — Department of Chemistry, University of Washington, Seattle, Washington 98195, United States
Chad E. Hoyer — Department of Chemistry, University of Washington, Seattle, Washington 98195, United States
Rahoul Banerjee Ghosh — Department of Chemistry,
University of Washington, Seattle, Washington 98195, United States

Andrew J. Jenkins — Department of Chemistry, University of Washington, Seattle, Washington 98195, United States;
orcid.org/0000-0002-1014-5225

Stefan Knecht — Algorithmiq Ltd, FI-00160 Helsinki, Finland; ETH Zürich, Department of Chemistry and Applied Life Sciences, CH-8093 Zürich, Switzerland; ◎ orcid.org/ 0000-0001-9818-2372

Michael J. Frisch — Gaussian Inc., Wallingford, Connecticut 06492, United States

Complete contact information is available at: https://pubs.acs.org/10.1021/acs.jpca.3c08031

#### Notes

The authors declare no competing financial interest.

## ACKNOWLEDGMENTS

This work was supported by the U.S. Department of Energy, Office of Science, Basic Energy Sciences, in the Heavy-Element Chemistry program (grant no. DE-SC0021100) for the development of variational relativistic multireference methods. The development of state interaction spin—orbit methods for computing excited-state couplings is supported by the Air Force Office of Scientific Research (grant no. FA9550-21-10344). Computations were facilitated through the use of advanced computational, storage, and networking infrastructure provided by the shared facility supported by the University of Washington Molecular Engineering Materials Center (DMR-2308979) via the Hyak supercomputer system.

#### REFERENCES

(1) Brissy, D.; Skander, M.; Retailleau, P.; Frison, G.; Marinetti, A. Platinum(II) Complexes Featuring Chiral Diphosphines and N-Heterocyclic Carbene Ligands: Synthesis and Evaluation as Cycloisomerization Catalysts. *Organometallics* **2009**, *28*, 140–151.

- (2) Xie, J.; Li, C.; Zhou, Q.; Wang, W.; Hou, Y.; Zhang, B.; Wang, X. Large Improvement in the Catalytic Activity Due to Small Changes in the Diimine Ligands: New Mechanistic Insight into the Dirhodium-(II,II) Complex-Based Photocatalytic H<sub>2</sub> Production. *Inorg. Chem.* **2012**, *51*, 6376–6384.
- (3) Dicken, R. D.; Motta, A.; Marks, T. J. Homoleptic Lanthanide Amide Catalysts for Organic Synthesis: Experiment and Theory. *ACS Catal.* **2021**, *11*, 2715–2734.
- (4) Esswein, A. J.; Nocera, D. G. Hydrogen Production by Molecular Photocatalysis. *Chem. Rev.* **2007**, *107*, 4022–4047.
- (5) Liao, C.; Zhu, M.; Jiang, D.-e.; Li, X. Manifestation of the Interplay Between Spin—Orbit and Jahn—Teller Effects in Au<sub>25</sub> Superatom UV-Vis Fingerprint Spectra. *Chem. Sci.* **2023**, *14*, 4666—4671.
- (6) Aguila, D.; Barrios, L. A.; Velasco, V.; Roubeau, O.; Repolles, A.; Alonso, P. J.; Sese, J.; Teat, S. J.; Luis, F.; Aromi, G. Heterodimetallic [LnLn'] Lanthanide Complexes: Toward a Chemical Design of Two-Qubit Molecular Spin Quantum Gates. *J. Am. Chem. Soc.* **2014**, *136*, 14215–14222.
- (7) van der Ende, B. M.; Aarts, L.; Meijerink, A. Lanthanide ions as spectral converters for solar cells. *Phys. Chem. Chem. Phys.* **2009**, *11*, 11081–11095.
- (8) Li, Z.; Leed, N. A.; Dickson-Karn, N. M.; Dunbar, K. R.; Turro, C. Directional Charge Transfer and Highly Reducing and Oxidizing Excited States of New Dirhodium(II,II) Complexes: Potential Applications in Solar Energy Conversion. *Chem. Sci.* **2014**, *5*, 727–737.
- (9) Roh, J. Y. D.; Smith, M. D.; Crane, M. J.; Biner, D.; Milstein, T. J.; Krämer, K. W.; Gamelin, D. R. Yb<sup>3+</sup> Speciation and Eenrgy-Transfer Dynamics in Quantum-Cutting Yb<sup>3+</sup>-Doped CsPbCl<sub>3</sub> Perovskite Nanocrystals and Single Crystals. *Phys. Rev. Mater.* **2020**, *4*. 105405.
- (10) Roos, B. O.; Taylor, P. R.; Sigbahn, P. E. A Complete Active Space SCF Method (CASSCF) Using a Density Matrix Formulated Super-CI Approach. *Chem. Phys.* **1980**, *48*, 157–173.
- (11) Heß, B. A.; Marian, C. M.; Wahlgren, U.; Gropen, O. A Meanfield Spin-orbit Method Applicable to Correlated Wavefunctions. *Chem. Phys. Lett.* **1996**, 251, 365–371.
- (12) Berning, A.; Schweizer, M.; Werner, H.-J.; Knowles, P. J.; Palmieri, P. Spin-Orbit Matrix Elements for Internally Contracted Multireference Configuration Interaction Wavefunctions. *Mol. Phys.* **2000**, *98*, 1823–1833.
- (13) Gagliardi, L.; Roos, B. O.; Malmqvist, P.-Å.; Dyke, J. M. On the Electronic Structure of the UO<sub>2</sub> Molecule. *J. Phys. Chem. A* **2001**, *105*, 10602–10606.
- (14) Koseki, S.; Fedorov, D. G.; Schmidt, M. W.; Gordon, M. S. Spin-Orbit Splittings in the Third-Row Transition Elements: Comparison of Effective Nuclear Charge and Full Breit-Pauli Calculations. J. Phys. Chem. A 2001, 105, 8262–8268.
- (15) Malmqvist, P. A.; Roos, B.; Schimmelpfennig, B. The Restricted Active Space (RAS) State Interaction Approach with Spin—Orbit Coupling. *Chem. Phys. Lett.* **2002**, *357*, 230—240.
- (16) Gagliardi, L.; Roos, B. O. The Electronic Spectrum of  $Re_2Cl_8^{2-}$ : A Theoretical Study. *Inorg. Chem.* **2003**, *42*, 1599–1603.
- (17) Roos, B. O.; Malmqvist, P.-Å. Relativistic Quantum Chemistry: The Multiconfigurational Approach. *Phys. Chem. Chem. Phys.* **2004**, *6*, 2919–2927.
- (18) Wang, F.; Ziegler, T. A Simplified Relativistic Time-Dependent Density-Functional Theory Formalism for the Calculations of Excitation Energies Including Spin-Orbit Coupling Effect. *J. Chem. Phys.* **2005**, *123*, 154102.
- (19) Klein, K.; Gauss, J. Perturbative Calculation of Spin-Orbit Splittings using the Equation-of-Motion Ionization-Potential Coupled-Cluster Ansatz. *J. Chem. Phys.* **2008**, *129*, 194106.
- (20) Wang, F.; Gauss, J.; van Wüllen, C. Closed-shell Coupled-cluster Theory with Spin-orbit Coupling. *J. Chem. Phys.* **2008**, *129*, 064113.
- (21) Wang, Z.; Wang, F. Spin-orbit Coupling and Electron Correlation at Various Coupled-cluster Levels for Closed-shell

- Diatomic Molecules. *Phys. Chem. Chem. Phys.* **2013**, *15*, 17922–17928.
- (22) Cheng, L.; Gauss, J. Perturbative Treatment of Spin-Orbit Coupling within Spin-Free Exact Two-Component Theory. *J. Chem. Phys.* **2014**, *141*, 164107.
- (23) Epifanovsky, E.; Klein, K.; Stopkowicz, S.; Gauss, J.; Krylov, A. Spin-Orbit Couplings within the Equation-of-Motion Coupled-Cluster Framework: Theory, Implementation, and Benchmark Calculations. *J. Chem. Phys.* **2015**, *143*, 064102.
- (24) Cheng, L.; Wang, F.; Stanton, J. F.; Gauss, J. Perturbative Treatment of Spin-orbit-coupling within Spin-free Exact Two-component Theory using Equation-of-motion Coupled-cluster Methods. J. Chem. Phys. 2018, 148, 044108.
- (25) Mussard, B.; Sharma, S. One-Step Treatment of Spin-Orbit Coupling and Electron Correlation in Large Active Spaces. *J. Chem. Theory Comput.* **2018**, *14*, 154–165.
- (26) Bokhan, D.; Trubnikov, D. N.; Perera, A.; Bartlett, R. J. Spin-orbit Split Ionized and Electron-attached States using Explicitly-Correlated Equation-of-motion Coupled-cluster Singles and Doubles Eigenvectors. *Chem. Phys. Lett.* **2019**, 730, 372–377.
- (27) Vidal, M. L.; Pokhilko, P.; Krylov, A. I.; Coriani, S. Equation-of-Motion Coupled-Cluster Theory to Model L-Edge X-ray Absorption and Photoelectron Spectra. *J. Phys. Chem. Lett.* **2020**, *11*, 8314–8321.
- (28) Meitei, O. R.; Houck, S. E.; Mayhall, N. J. Spin-Orbit Matrix Elements for a Combined Spin-Flip and IP/EA Approach. *J. Chem. Theory Comput.* **2020**, *16*, 3597–3606.
- (29) Carreras, A.; Jiang, H.; Pokhilko, P.; Krylov, A. I.; Zimmerman, P. M.; Casanova, D. Calculation of Spin-orbit Couplings using RASCI Spinless One-particle Density Matrices: Theory and Applications. *J. Chem. Phys.* **2020**, *153*, 214107.
- (30) Liao, C.; Kasper, J. M.; Jenkins, A. J.; Yang, P.; Batista, E. R.; Frisch, M. J.; Li, X. State Interaction Linear Response Time-Dependent Density Functional Theory with Perturbative Spin—Orbit Coupling: Benchmark and Perspectives. *JACS Au* 2023, 3, 358–367.
- (31) Gagliardi, L.; Roos, B. O. Quantum Chemical Calculations Show That the Uranium Molecule  $U_2$  Has a Quintuple Bond. *Nature* **2005**, 433, 848–851.
- (32) Knecht, S.; Jensen, H. J. A.; Saue, T. Relativistic Quantum Chemical Calculations Show That the Uranium Molecule  $U_2$  Has a Quadruple Bond. *Nat. Chem.* **2019**, *11*, 40–44.
- (33) Ciborowski, S. M.; Mitra, A.; Harris, R. M.; Liu, G.; Sharma, P.; Khetrapal, N.; Blankenhorn, M.; Gagliardi, L.; Bowen, K. H. Metal-Metal Bonding in Actinide Dimers: U<sub>2</sub> and U<sub>2</sub><sup>-</sup>. *J. Am. Chem. Soc.* **2021**, *143*, 17023–17028.
- (34) Mohanty, A.; Clementi, E. Dirac-Fock Self-Consistent Field Method for Closed-Shell Molecules with Kinetic Balance and Finite Nuclear Size. *Int. J. Quantum Chem.* **1991**, *39*, 487–517.
- (35) Eliav, E.; Kaldor, U. The Relativistic Four-Component Coupled Cluster Method for Molecules: Spectroscopic Constants of SnH4. *Chem. Phys. Lett.* **1996**, 248, 405–408.
- (36) Visscher, L.; Lee, T. J.; Dyall, K. G. Formulation and Implementation of a Relativistic Unrestricted Coupled-Cluster Method Including Noniterative Connected Triples. *J. Chem. Phys.* **1996**, *105*, 8769–8776.
- (37) Jo/rgen Aa Jensen, H.; Dyall, K. G.; Saue, T.; Faegri, K., Jr Relativistic Four-Component Multiconfigurational Self-Consistent-Field Theory for Molecules: Formalism. *J. Chem. Phys.* **1996**, *104*, 4083–4097.
- (38) Saue, T.; Faegri, K.; Helgaker, T.; Gropen, O. Principles of Direct 4-Component Relativistic SCF: Application to Caesium Auride. *Mol. Phys.* **1997**, *91*, 937–950.
- (39) Saue, T.; Fægri, K.; Helgaker, T.; Gropen, O. Principles of direct 4-component relativistic SCF: application to caesium auride. *Mol. Phys.* **1997**, *91*, *937*–*950*.
- (40) Fleig, T.; Olsen, J.; Visscher, L. The Generalized Active Space Concept for the Relativistic Treatment of Electron Correlation. II. Large-Scale Configuration Interaction Implementation Based on Relativistic 2- and 4-Spinors and its Application. *J. Chem. Phys.* **2003**, *119*, 2963–2971.

- (41) Gao, J.; Liu, W.; Song, B.; Liu, C. Time-Dependent Four-Component Relativistic Density Functional Theory for Excitation Energies. *J. Chem. Phys.* **2004**, 121, 6658–6666.
- (42) Gao, J.; Zou, W.; Liu, W.; Xiao, Y.; Peng, D.; Song, B.; Liu, C. Time-Dependent Four-Component Relativistic Density-Functional Theory for Excitation Energies. II. The Exchange-Correlation Kernel. *J. Chem. Phys.* **2005**, *123*, 054102.
- (43) Fleig, T.; Jensen, H. J. A.; Olsen, J.; Visscher, L. The Generalized Active Space Concept for the Relativistic Treatment of Electron Correlation. III. Large-Scale Configuration Interaction and Multiconfiguration Self-Consistent-Field Four-Component Methods with Application to UO2. *J. Chem. Phys.* **2006**, *124*, 104106.
- (44) Dyall, K. G.; Faegri, K. Introduction to Relativistic Quantum Chemistry; Oxford University Press, Inc., 2007.
- (45) Thyssen, J.; Fleig, T.; Jensen, H. J. A. A Direct Relativistic Four-Component Multiconfiguration Self-Consistent-Field Method for Molecules. *I. Chem. Phys.* **2008**, *129*, 034109.
- (46) Sørensen, L. K.; Knecht, S.; Fleig, T.; Marian, C. M. Four-Component Relativistic Coupled Cluster and Configuration Interaction Calculations on the Ground and Excited States of the RbYb Molecule. *J. Phys. Chem. A* **2009**, *113*, 12607–12614.
- (47) Saue, T. Relativistic Hamiltonians for Chemistry: A Primer. ChemPhysChem 2011, 12, 3077-3094.
- (48) Reiher, M.; Wolf, A. Relativistic Quantum Chemistry, 2nd ed.; Wiley VCH, 2015.
- (49) Bates, J. E.; Shiozaki, T. Fully Relativistic Complete Active Space Self-Consistent Field for Large Molecules: Quasi-Second-Order Minimax Optimization. *J. Chem. Phys.* **2015**, *142*, 044112.
- (50) Zhang, B.; Vandezande, J. E.; Reynolds, R. D.; Schaefer, H. F., III Spin-Orbit Coupling via Four-Component Multireference Methods: Benchmarking on p-Block Elements and Tentative Recommendations. J. Chem. Theory Comput. 2018, 14, 1235–1246.
- (51) Egidi, F.; Sun, S.; Goings, J. J.; Scalmani, G.; Frisch, M. J.; Li, X. Two-Component Non-Collinear Time-Dependent Spin Density Functional Theory for Excited State Calculations. *J. Chem. Theory Comput.* **2017**, *13*, 2591–2603.
- (52) Hu, H.; Jenkins, A. J.; Liu, H.; Kasper, J. M.; Frisch, M. J.; Li, X. Relativistic Two-Component Multireference Configuration Interaction Method with Tunable Correlation Space. *J. Chem. Theory Comput.* **2020**, *16*, 2975–2984.
- (53) Liu, J.; Cheng, L. Relativistic Coupled-Cluster and Equation-of-Motion Coupled-Cluster Methods. Wiley Interdiscip. Rev.: Comput. Mol. Sci. 2021, 11, 1536.
- (54) Hoyer, C. E.; Li, X. Relativistic Two-Component Projection-Based Quantum Embedding for Open-Shell Systems. *J. Chem. Phys.* **2020**, *153*, 094113.
- (55) Grofe, A.; Gao, J.; Li, X. Exact-Two-Component Block-Localized Wave Function: A Simple Scheme for the Automatic Computation of Relativistic  $\Delta$ SCF. J. Chem. Phys. **2021**, 155, 014103.
- (56) Sharma, P.; Jenkins, A. J.; Scalmani, G.; Frisch, M. J.; Truhlar, D. G.; Gagliardi, L.; Li, X. Exact-Two-Component Multiconfiguration Pair-Density Functional Theory. *J. Chem. Theory Comput.* **2022**, *18*, 2947–2954.
- (57) Grofe, A.; Li, X. Relativistic Nonorthogonal Configuration Interaction: Application to L<sub>2,3</sub>-edge X-ray Spectroscopy. *Phys. Chem. Chem. Phys.* **2022**, *24*, 10745–10756.
- (58) Lu, L.; Hu, H.; Jenkins, A. J.; Li, X. Exact-Two-Component Relativistic Multireference Second-Order Perturbation Theory. *J. Chem. Theory Comput.* **2022**, *18*, 2983–2992.
- (59) Hoyer, C. E.; Hu, H.; Lu, L.; Knecht, S.; Li, X. Relativistic Kramers-Unrestricted Exact-Two-Component Density Matrix Renormalization Group. *J. Phys. Chem. A* **2022**, *126*, 5011–5020.
- (60) Hoyer, C. E.; Lu, L.; Hu, H.; Shumilov, K. D.; Sun, S.; Knecht, S.; Li, X. Correlated Dirac—Coulomb—Breit Multiconfigurational Self-Consistent-Field Methods. *I. Chem. Phys.* **2023**. *158*, 044101.
- (61) Dyall, K. G. Interfacing Relativistic and Nonrelativistic Methods. I. Normalized Elimination of the Small Component in the Modified Dirac Equation. *J. Chem. Phys.* **1997**, *106*, 9618–9626.

- (62) Dyall, K. G. Interfacing Relativistic and Nonrelativistic Methods. II. Investigation of a Low-Order Approximation. *J. Chem. Phys.* **1998**, *109*, 4201–4208.
- (63) Dyall, K. G.; Enevoldsen, T. Interfacing Relativistic and Nonrelativistic Methods. III. Atomic 4-Spinor Expansions and Integral Approximations. *J. Chem. Phys.* **1999**, *111*, 10000–10007.
- (64) Dyall, K. G. Interfacing relativistic and nonrelativistic methods. IV. One- and two-electron scalar approximations. *J. Chem. Phys.* **2001**, *115*, 9136–9143.
- (65) Filatov, M.; Cremer, D. A New Quasi-Relativistic Approach for Density Functional Theory Based on the Normalized Elimination of the Small Component. *Chem. Phys. Lett.* **2002**, *351*, 259–266.
- (66) Kutzelnigg, W.; Liu, W. Quasirelativistic Theory Equivalent to Fully Relativistic Theory. *J. Chem. Phys.* **2005**, 123, 241102.
- (67) Liu, W.; Peng, D. Infinite-Order Quasirelativistic Density Functional Method Based on the Exact Matrix Quasirelativistic Theory. *J. Chem. Phys.* **2006**, 125, 044102.
- (68) Peng, D.; Liu, W.; Xiao, Y.; Cheng, L. Making Four- and Two-Component Relativistic Density Functional Methods Fully Equivalent Based on the Idea of From Atoms to Molecule. *J. Chem. Phys.* **2007**, 127, 104106.
- (69) Ilias, M.; Saue, T. An infinite-order two-component relativistic Hamiltonian by a simple one-step transformation. *J. Chem. Phys.* **2007**, *126*, 064102.
- (70) Liu, W.; Peng, D. Exact Two-component Hamiltonians Revisited. J. Chem. Phys. 2009, 131, 031104.
- (71) Liu, W. Ideas of Relativistic Quantum Chemistry. *Mol. Phys.* **2010**, *108*, 1679–1706.
- (72) Li, Z.; Xiao, Y.; Liu, W. On the Spin Separation of Algebraic Two-Component Relativistic Hamiltonians. *J. Chem. Phys.* **2012**, *137*, 154114.
- (73) Peng, D.; Middendorf, N.; Weigend, F.; Reiher, M. An Efficient Implementation of Two-Component Relativistic Exact-Decoupling Methods for Large Molecules. *J. Chem. Phys.* **2013**, *138*, 184105.
- (74) Egidi, F.; Goings, J. J.; Frisch, M. J.; Li, X. Direct Atomic-Orbital-Based Relativistic Two-Component Linear Response Method for Calculating Excited-State Fine Structures. *J. Chem. Theory Comput.* **2016**, *12*, 3711–3718.
- (75) Goings, J. J.; Kasper, J. M.; Egidi, F.; Sun, S.; Li, X. Real Time Propagation of the Exact Two Component Time-Dependent Density Functional Theory. *J. Chem. Phys.* **2016**, *145*, 104107.
- (76) Konecny, L.; Kadek, M.; Komorovsky, S.; Malkina, O. L.; Ruud, K.; Repisky, M. Acceleration of Relativistic Electron Dynamics by Means of X2C Transformation: Application to the Calculation of Nonlinear Optical Properties. *J. Chem. Theory Comput.* **2016**, *12*, 5823–5833.
- (77) Jenkins, A. J.; Liu, H.; Kasper, J. M.; Frisch, M. J.; Li, X. Variational Relativistic Two-Component Complete-Active-Space Self-Consistent Field Method. *J. Chem. Theory Comput.* **2019**, *15*, 2974–2982.
- (78) Ganyushin, D.; Neese, F. A Fully Variational Spin-Orbit Coupled Complete Active Space Self-Consistent Field Approach: Application to Electron Paramagnetic Resonance g-Tensors. *J. Chem. Phys.* **2013**, *138*, 104113.
- (79) Berning, A. Spin-Orbit Matrix Elements for Internally Contracted Multireference Configuration Interaction Wavefunctions. *Mol. Phys.* **2000**, *98*, 1823.
- (80) Fedorov, D. G.; Gordon, M. S. A Study of the Relative Importance of One and Two-Electron Contributions to Spin-Orbit Coupling. *J. Chem. Phys.* **2000**, *112*, 5611–5623.
- (81) Li, Z.; Suo, B.; Zhang, Y.; Xiao, Y.; Liu, W. Combining Spin-Adapted Open-Shell TD-DFT with Spin-Orbit Coupling. *Mol. Phys.* **2013**, *111*, 3741–3755.
- (82) Malmqvist, P. A. Calculation of Transition Density Matrices by Nonunitary Orbital Transformations. *Int. J. Quantum Chem.* **1986**, *30*, 479–494.
- (83) Malmqvist, P. A.; Roos, B. The CASSCF State Interaction Method. Chem. Phys. Lett. 1989, 155, 189–194.

- (84) Li Manni, G.; Fdez Galván, I.; Alavi, A.; Aleotti, F.; Aquilante, F.; Autschbach, J.; Avagliano, D.; Baiardi, A.; Bao, J. J.; Battaglia, S.; Birnoschi, L.; Blanco-González, A.; Bokarev, S. I.; Broer, R.; Cacciari, R.; Calio, P. B.; Carlson, R. K.; Carvalho Couto, R.; Cerdán, L.; Chibotaru, L. F.; Chilton, N. F.; Church, J. R.; Conti, I.; Coriani, S.; Cuéllar-Zuquin, J.; Daoud, R. E.; Dattani, N.; Decleva, P.; de Graaf, C.; Delcey, M. G.; De Vico, L.; Dobrautz, W.; Dong, S. S.; Feng, R.; Ferré, N.; Filatov(Gulak), M.; Gagliardi, L.; Garavelli, M.; González, L.; Guan, Y.; Guo, M.; Hennefarth, M. R.; Hermes, M. R.; Hoyer, C. E.; Huix-Rotllant, M.; Jaiswal, V. K.; Kaiser, A.; Kaliakin, D. S.; Khamesian, M.; King, D. S.; Kochetov, V.; Krośnicki, M.; Kumaar, A. A.; Larsson, E. D.; Lehtola, S.; Lepetit, M.-B.; Lischka, H.; López Ríos, P.; Lundberg, M.; Ma, D.; Mai, S.; Marquetand, P.; Merritt, I. C. D.; Montorsi, F.; Mörchen, M.; Nenov, A.; Nguyen, V. H. A.; Nishimoto, Y.; Oakley, M. S.; Olivucci, M.; Oppel, M.; Padula, D.; Pandharkar, R.; Phung, Q. M.; Plasser, F.; Raggi, G.; Rebolini, E.; Reiher, M.; Rivalta, I.; Roca-Sanjuán, D.; Romig, T.; Safari, A. A.; Sánchez-Mansilla, A.; Sand, A. M.; Schapiro, I.; Scott, T. R.; Segarra-Martí, J.; Segatta, F.; Sergentu, D.-C.; Sharma, P.; Shepard, R.; Shu, Y.; Staab, J. K.; Straatsma, T. P.; Sørensen, L. K.; Tenorio, B. N. C.; Truhlar, D. G.; Ungur, L.; Vacher, M.; Veryazov, V.; Voß, T. A.; Weser, O.; Wu, D.; Yang, X.; Yarkony, D.; Zhou, C.; Zobel, J. P.; Lindh, R. The OpenMolcas Web: A Community-Driven Approach to Advancing Computational Chemistry. J. Chem. Theory Comput. 2023, 19, 6933-6991.
- (85) Dyall, K. G. An Exact Separation of the Spin-Free and Spin-Dependent Terms of the Dirac-Coulomb-Breit Hamiltonian. *J. Chem. Phys.* **1994**, *100*, 2118–2127.
- (86) Sun, S.; Ehrman, J.; Zhang, T.; Sun, Q.; Dyall, K. G.; Li, X. Scalar Breit Interaction for Molecular Calculations. *J. Chem. Phys.* **2023**, *158*, 171101.
- (87) Boettger, J. C. Approximate Two-Electron Spin-Orbit Coupling Term for Density-Functional-Theory DFT Calculations Using the Douglas-Kroll-Hess Transformation. *Phys. Rev. B* **2000**, *62*, 7809–7815.
- (88) Ehrman, J.; Martinez-Baez, E.; Jenkins, A. J.; Li, X. Improving One-Electron Exact-Two-Component Relativistic Methods with the Dirac-Coulomb-Breit-Parameterized Effective Spin-Orbit Coupling. J. Chem. Theory Comput. 2023, 19, 5785-5790.
- (89) Liu, J.; Cheng, L. An atomic mean-field spin-orbit approach within exact two-component theory for a non-perturbative treatment of spin-orbit coupling. *J. Chem. Phys.* **2018**, *148*, 144108.
- (90) Frisch, M. J.; Trucks, G. W.; Schlegel, H. B.; Scuseria, G. E.; Robb, M. A.; Cheeseman, J. R.; Scalmani, G.; Barone, V.; Petersson, G. A.; Nakatsuji, H.; Li, X.; Caricato, M.; Marenich, A. V.; Bloino, J.; Janesko, B. G.; Gomperts, R.; Mennucci, B.; Hratchian, H. P.; Ortiz, J. V.; Izmaylov, A. F.; Sonnenberg, J. L.; Williams-Young, D.; Ding, F.; Lipparini, F.; Egidi, F.; Goings, J.; Peng, B.; Petrone, A.; Henderson, T.; Ranasinghe, D.; Zakrzewski, V. G.; Gao, J.; Rega, N.; Zheng, G.; Liang, W.; Hada, M.; Ehara, M.; Toyota, K.; Fukuda, R.; Hasegawa, J.; Ishida, M.; Nakajima, T.; Honda, Y.; Kitao, O.; Nakai, H.; Vreven, T.; Throssell, K.; Montgomery, J. A., Jr; Peralta, J. E.; Ogliaro, F.; Bearpark, M. J.; Heyd, J. J.; Brothers, E. N.; Kudin, K. N.; Staroverov, V. N.; Keith, T. A.; Kobayashi, R.; Normand, J.; Raghavachari, K.; Rendell, A. P.; Burant, J. C.; Iyengar, S. S.; Tomasi, J.; Cossi, M.; Millam, J. M.; Klene, M.; Adamo, C.; Cammi, R.; Ochterski, J. W.; Martin, R. L.; Morokuma, K.; Farkas, O.; Foresman, J. B.; Fox, D. J. Gaussian Development Version. Revision J.14+; Gaussian, Inc.: Wallingford, CT, 2021.
- (91) Sjøvoll, M.; Fagerli, H.; Gropen, O.; Almlöf, J.; Schimmelpfennig, B.; Wahlgren, U. An Efficient Treatment of Kinematic Factors in Pseudo-Relativistic Calculations of Electronic Structure. *Theor. Chem. Acc.* **1998**, 99, 1–7.
- (92) Jung, J.; Atanasov, M.; Neese, F. Ab Initio Ligand-Field Theory Analysis and Covalency Trends in Actinide and Lanthanide Free Ions and Octahedral Complexes. *Inorg. Chem.* **2017**, *56*, 8802–8816.
- (93) Roos, B. O.; Lindh, R.; Malmqvist, P.-A.; Veryazov, V.; Widmark, P.-O. Main Group Atoms and Dimers Studied with a New Relativistic ANO Basis Set. *J. Phys. Chem. A* **2004**, *108*, 2851–2858.

- (94) Pritchard, B. P.; Altarawy, D.; Didier, B.; Gibson, T. D.; Windus, T. L. New Basis Set Exchange: An Open, Up-to-Date Resource for the Molecular Sciences Community. *J. Chem. Inf. Model.* **2019**, *59*, 4814–4820.
- (95) Nicklass, A.; Peterson, K. A.; Berning, A.; Werner, H.-J.; Knowles, P. J. Convergence of Breit–Pauli spin–orbit matrix elements with basis set size and configuration interaction space: The halogen atoms F, Cl, and Br. J. Chem. Phys. 2000, 112, 5624–5632.
- (96) VanGundy, R. A.; Persinger, T. D.; Heaven, M. C. Low Energy States of NdO<sup>+</sup> Probed by Photoelectron Spectroscopy. *J. Chem. Phys.* **2019**, *150*, 114302.
- (97) Sun, S.; Stetina, T. F.; Zhang, T.; Hu, H.; Valeev, E. F.; Sun, Q.; Li, X. Efficient Four-Component Dirac—Coulomb—Gaunt Hartree—Fock in the Pauli Spinor Representation. *J. Chem. Theory Comput.* **2021**, *17*, 3388—3402.
- (98) Sun, S.; Ehrman, J. N.; Sun, Q.; Li, X. Efficient Evaluation of the Breit Operator in the Pauli Spinor Basis. *J. Chem. Phys.* **2022**, *157*, 064112.